Conformational Mobility of Oligosaccharides: Experimental Evidence for the Existence of an "Anti" Conformer of the Galβ1-3Glcβ1-OMe Disaccharide

Janusz Dabrowski,* Tibor Kožár,† Horst Grosskurth, and Nicolay E. Nifant'ev‡

Contribution from the Max Planck Institute for Medical Research, D-69120 Heidelberg, Germany

Received September 6, 1994[⊗]

Abstract: A hydrogen bond between the Glc OH(4) and Gal OH(2) groups of the title disaccharide, manifested by the doubling of their ^{1}H NMR signals in a partially deuteriated sample in Me_2SO solution, proves the existence of an "*anti*" conformer, i.e., one with the anomeric and transglycosidic aglyconic C−H bonds turned away from each other by ~180°. This conformer is at equilibrium with the predominating normal "*syn*" conformation(s), as shown by the analysis of several interresidue NOEs, and confirmed by molecular mechanics and molecular dynamics calculations.

Introduction

Oligosaccharides and polysaccharides are ubiquitous in Nature and perform important functions in countless biological processes. Their three-dimensional structure, or conformation, is considered essential in molecular recognition, e.g., in antigen−antibody interactions; however, it is unpredictable as to whether the conformations fixed in complexes with receptors will be the same as those that were observed in solution.[1] Consequently, the rigidity *vs* flexibility of oligosaccharide chains is an issue of great interest, because it concerns the potential adaptability of saccharides to the spatial and electronic requirements of the receptor. Although absolute rigidity can obviously be ruled out, the views concerning the degree of flexibility vary widely, ranging from the acceptance of only restricted fluctuations around a preferred conformation[2] to the admission of wide-range variability of both the glycosidic angles Φ and Ψ (for their definition, see Methods).[2f,g,3] In particular, the "*anti*" conformations (with the transglycosidic C−H bonds turned from each other by ~180°, as in Figure 4b), whose presence would mean maximum flexibility, have never been observed in HSEA (hard-sphere exo-anomeric)[4] or related (GESA,[5] HEAH,[6] HSEL[6]) calculations, although they have often been obtained with the use of other force fields.[2f,g,3a,7] Experimental data supporting the existence of an *anti* conformation (Φ or Ψ ~180°) are scarce and mostly ambiguous, for example, for DGlcβ1-4-LRhaα1-OMe,[7b] where the critical NOEs observed were for mutually strongly coupled protons, or in the case of cellobiose,[3a] where the weak, additional NOEs observed could be alternatively explained in terms of a slightly deformed *syn* conformation. Recently, however, an appreciable percentage of the *anti* conformation for a thioglycosidic linkage in methyl 4-thio-β-maltoside was found experimentally by Bock et al.[3e] and confirmed by hard sphere calculations, without inclusion of the exo-anomeric term. Although the experimental evidence given is convincing, this result has no direct bearing upon conformations of normal, unmodified oligosaccharides, because the C−S−C thioglycosidic linkage places the two neighboring sugar rings at a distance larger by ca. 0.4 Å than does the C−O−C linkage, thus substantially reducing most of the attractive and repulsive interresidue interactions that usually restrict the conformational mobility of the molecule. Similarly, the *anti* conformation observed in the same study[3e] for a NH-bridged, protonated disaccharide depends on structural factors completely different from those characteristic of usual oligosaccharides. In a study from this laboratory,[3c] the *anti* conformation of the Galβ1-4Glcβ segment of globoside was strongly substantiated by a rotating frame NOE contact between protons OH3 of Glc and OH2 of Gal in Me_2SO-d_6 solution. Generally, however, many sources of errors, such as experimental inaccuracies, HOHAHA-type (homonuclear Hartmann-Hahn) transfer of magnetization and relayed NOE,[8a] strong coupling,[8b] improper

* To whom correspondence should be addressed.

† On leave of absence from the Institute of Experimental Physics, Slovak Academy of Sciences, Košice, Slovak Republic.

‡ Permanent address: Zelinsky Institute of Organic Chemistry, Russian Academy of Sciences, Moscow, Russia.

[⊗] Abstract published in *Advance ACS Abstracts*, May 1, 1995.

(1) (a) Glaudemans, C. P. J.; Lerner, L.; Daves Jr., G. D.; Kovác, P.; Venable, R.; Bax, A. *Biochemistry* **1990**, *29*, 10906−10911. (b) Bevilacqua, V. L.; Kim, Y.; Prestegard, J. H. *Biochemistry* **1992**, *31*, 9339−9349. (c) Carver, J. P. *Pure Appl. Chem.* **1993**, *65*, 763−770. (d) Weimar, T.; Peters, T. *Angew. Chem.* **1994**, *106*, 79−82. (e) Bundle, D. R.; Bauman, H.; Brisson, J.-R.; Gagné, M.; Zdanow, A.; Cygler, M. *Biochemistry* **1994**, *33*, 5183−5192.

(2) (a) Spohr, U.; Lemieux, R. U. *Carbohydr. Res.* **1988**, *174*, 211−237. (b) Jansson, P.-E.; Kenne, L.; Schweda, E. *J. Chem. Soc. Perkin Trans. 1* **1988**, 2729−2736. (c) Kline, P. C.; Serianni, A. S.; Huang, S.-G.; Hayes, M.; Barker, R. *Can. J. Chem.* **1990**, *68*, 2177−2182. (d) Scarsdale, J. N.; Prestegard, J. H.; Yu, R. K. *Biochemistry* **1990**, *29*, 9843−9855. (e) Edge, C. J.; Singh, U. C.; Bazzo, R.; Taylor, G. L.; Dwek, R. A.; Rademacher, T. W. *Biochemistry* **1990**, *29*, 1971−1974. (f) Yan, Z.-Y.; Bush, C. A. *Biopolymers* **1990**, *29*, 799−811. (g) Mukhopadhyay, C.; Bush, C. A. *Biopolymers* **1991**, *31*, 1737−1746. (h) Cagas, P.; Bush, C. A. *Biopolymers* **1992**, *32*, 277−292. (i) Rutheford, T. J.; Partridge, J.; Weller, C. T.; Homans, S. W. *Biochemistry* **1993**, *32*, 12715−12724.

(3) (a) Lipkind, G. M.; Shashkov, A. S.; Kochetkov, N. K. *Carbohydr. Res.* **1985**, *141*, 191−197. (b) Breg, J.; Kroon-Batenburg, L. M. J.; Strecker, G.; Montreuil, J.; Vliegenthart, J. F. G. *Eur. J. Biochem.* **1989**, *178*, 727−739. (c) Poppe, L.; Lieth, C.-W., v. d.; Dabrowski, J. *J. Am. Chem. Soc.* **1990**, *112*, 7762−7771. (d) Bechtel, B.; Wand, A. J.; Wroblewski, K.; Koprowski, H.; Turin, J. *J. Biol. Chem.* **1990**, *265*, 2028−2037. (e) Bock, K.; Duus, J. Ø; Refn, S. *Carbohydr. Res.* **1994**, *253*, 51−67. Asensio, J. L.; Jimenez-Barbero, J. *Biopolymers* **1995**, *35*, 55−73.

(4) (a) Lemieux, R. U.; Bock, K.; Delbaere, L. T. J.; Koto, S.; Rao, V. S. *Can. J. Chem.* **1980**, *58*, 631−653. (b) Thøgersen, H.; Lemieux, R. U.; Bock, K.; Meyer, B. *Can. J. Chem.* **1982**, *60*, 44−57.

(5) Paulsen, H.; Peters, T.; Sinwell, V.; Lebuhn, R.; Meyer, B. *Justus Liebigs Ann. Chem.* **1985**, 489−509.

(6) Cumming, D. A.; Carver, J. P. *Biochemistry* **1987**, *26*, 6664−6676.

(7) (a) Melberg, S.; Rasmussen, K. *Carbohydr. Res.* **1979**, *69*, 27−38, and **1980**, *78*, 215−224. (b) Lipkind, G. M.; Shashkov, A. S.; Nikolaev, A. V.; Mamyan, S. S.; Kochetkov, N. K. *Bioorg. Khim.* **1987**, *13*, 1081−1092. (c) Ha, S. N.; Madsen, L. J.; Brady, J. W. *Biopolymers* **1988**, *27*, 1927−1952. (d) Choe, B.-Y.; Ekborg, G. C.; Rodén, L.; Harvey, S. C.; Krishna, N. R. *J. Am. Chem. Soc.* **1991**, *113*, 3743−3749. (e) Rambaud, E.; Buléon, A.; Pérez, S. *Carbohydr. Res.* **1992**, *227*, 351−363.

0002-7863/95/1517-5534$09.00/0

averaging due to internal motion,[8c] proton exchange,[8d,9] etc., must be taken into account when using NOE-derived distances as constraints in conformational analysis. Moreover, a principal difficulty with NOE is its averaging over distances between the given interacting protons in the case of fast equilibrating flexible molecules. For this reason, the conformations derived from NOE, and other NMR observables for that matter (coupling constants, chemical shifts, relaxation), are virtual,[6,10] so that resolving of such apparent conformations into real components remains the central problem of conformational analysis.

In contrast, reliably established hydrogen bonds are fundamentally different, in that they provide fairly precise, *non-averaged* constraints, with the upper limit of the corresponding O···O distance of 3 Å and a very small margin of uncertainty.[11] If such a H-bond distance constraint delimits a region in conformational space that is clearly separated from other firmly determined regions (for example, the region determined by NOE for the transglycosidic anomeric/aglyconic proton pair), there can be no doubt about pronounced flexibility involving the existence of different interconverting conformers. Most importantly, such confidently established separate regions in the conformational space of a molecule can serve as a test for the validity of force fields used in theoretical calculations.

Direct proof of a hydrogen bond between two OH groups is additional splitting of their ^{1}H NMR signals after partial deuteration, due to the coexistence of the ROH···O(H)R′ and ROH···O(D)R′ isotopomers (where R and R′ are the neighboring sugar residues).[12] Such phenomena are best observed in dimethyl sulfoxide, which enables one to obtain well resolved, unbroadened OH signals.

Apart from the application of OH signals for the observation of such H/D isotope effects, they can also be used as an additional source of NOE distance information. Since the hydroxyl protons range over a twice larger distance from the sugar skeleton than the C-linked protons do, they show many more interresidue NOEs that enable one to better determine the conformation, or conformational equilibrium, of the system studied.[3c,9,13] Because only very weak NOEs were observed in laboratory-frame spectra, and in order to be able to distinguish NOEs from exchange signals, we measured rotating-frame NOE spectra (CAMELSPIN,[14] ROESY). The problems arising from possible ROESY artifacts will be dealt with in the following sections.

Materials and Methods

Methyl 3-β-D-galactosyl-β-D-glucopyranoside (**1**) was obtained as described previously.[15]

For assignments and ROE measurements, a solution was prepared from a 12 mg sample of **1**, which was dried under high vacuum and dissolved in 0.4 mL Me_2SO-d_6 purchased from Merck, Darmstadt. Partially deuterated **1** was obtained in the same solution by adding a calculated amount of D_2O.

NMR Measurements. All spectra were obtained at the frequency of 500 MHz with a Bruker AM-500 spectrometer. Chemical shifts were referenced indirectly to Me_4Si, by setting the ^{1}H signal of residual Me_2SO-d_5 at 2.50 ppm.

Assignments were obtained, and coupling constants measured, with the aid of two-dimensional (2D) phase-sensitive COSY (Bruker Software, digital resolution 0.3 Hz per point) and 1D HOHAHA spectra. For the latter, a selective excitation with a DANTE pulse[16] was applied, followed by a MLEV-17 pulse sequence for spin lock,[17] and a z-filter for purging phase distortions.[17,18] The mixing time was 200 ms.

The isotope effect was observed in a conventional 1D spectrum recorded with a digital resolution of 0.18 Hz/pt. The 2D ROESY spectra were recorded in the phase-sensitive mode with use of the TPPI method. A Hahn-echo pulse sequence was applied before acquisition,[19] and the receiver was adjusted to the absorption mode[20] for avoiding baseline distortion. The pulse sequence advanced by Rance[21] was used, a train of ~20° pulses[22] sandwiched by two 170° pulses[23] and two z-filters being executed during the mixing time of 200 ms. The rf carrier frequency was placed about 1 kHz downfield relative to the center of proton resonances and at the center during evolution and acquisition. The effective field for spin-locking was 2.5 kHz. A total of 512 free induction decays (FIDs), 96 scans each, were accumulated with a repetition time of 2.5 s. All 2D time domain spectra were zero filled, multiplied by a squared cosine bell function, and Fourier transformed to give a final resolution of 0.6 Hz/pt in ω_2 and 1.2 Hz/pt in ω_1. Transient 1D ROESY experiments were performed with DANTE excitation, 300 ms mixing time, direct subtraction of reference FIDs every eight scans, and accumulations of a total of 8000 scans per spectrum.

Distance-Mapping. The main conformational feature—the mutual orientation of neighboring sugar residues, is described by the glycosidic angles $\Phi = \angle(H1-C1-O1-C_x)$ and $\Psi = \angle(C1-O1-C_x-H_x)$, where C_x and H_x are the aglyconic atoms. Φ is defined as positive by the clockwise rotation of the $O1-C_x$ bond, while viewing from the fixed $H1-C1$ bond along the $C1-O1$ rotation axis; with eclipsed $H1-C1$ and $O1-C_x$ bonds, $\Phi = 0$. A positive Ψ angle is defined by the clockwise rotation of the C_x-H_x bond, while viewing from the fixed $C1-O1$ bond along the $O1-C_x$ rotation axis; with eclipsed $C1-O1$ and C_x-H_x bonds, $\Psi = 0$. The dihedral angles of secondary hydroxy groups are defined similarly for the H−O−C−H bond sequence. The three rotamers are designed as *trans* (*t*) (180°), *gauche*$^+$ (g^+) (60°), and *gauche*$^-$ (g^-) (−60°).[24]

Our approach of using distance constraints in conformational analysis has been described in detail,[3c] hence only some points of relevance here will be briefly recapitulated. We use NOE-based distances for both the C- and O-linked protons, and consider them as upper distance limits for one of the conformations at equilibrium, the lower limit being the sum of van der Waals radii or the minimum distance determined by covalent geometry. For O-linked protons, "effective distances" allowing for the rotamers' distribution (Figure 2) are calculated on the

(8) (a) Neuhaus, D.; Williamson, M. P. *The Nuclear Overhauser Effect in Structural and Conformational Analysis*; VCH Publishers, New York, 1989; pp 318−327. (b) pp 194−203. (c) pp 170−175. (d) pp 148−160.
(9) Dabrowski, J.; Poppe, L. *J. Am. Chem. Soc.* **1989**, *111*, 1510−1511.
(10) Jardetzky, O. *Biochim. Biophys. Acta* **1980**, *621*, 227−232.
(11) Jeffrey, G. A.; Saenger, W. *Hydrogen Bonding in Biological Structures*; Springer, Berlin, 1991.
(12) (a) Lemieux, R. U.; Bock, K. *Jpn. J. Antibiot. Suppl.* **1979**, *32*, 163−177. (b) Christofides, J. C.; Davies, D. B. *J. Chem. Soc., Chem. Commun.* **1982**, 560−562. (c) Reuben, J. *J. Am. Chem. Soc.* **1984**, *106*, 6180−6186.
(13) Dabrowski, U.; Dabrowski, J.; Grosskurth, H.; Lieth, C.-W. v. d.; Ogawa, T. *Biochem. Biophys. Res. Commun.* **1993**, *192*, 1057−1065.
(14) Bothner-By, A. A.; Stephens, R. L.; Lee, J.; Warren, C. D.; Jeanloz, R. W. *J. Am. Chem. Soc.* **1984**, *106*, 811−813.
(15) (a) Nifant'ev, N. E.; Amochaeva, V. Y.; Shashkov, A. S.; Kochetkov, N. K. *Carbohydr. Res.* **1993**, *250*, 211−230. (b) Shashkov, A. S.; Nifant'ev, N. E.; Amochaeva, V. Y.; Kochetkov, N. K. *Magn. Reson. Chem.* **1993**, *31*, 599−605.
(16) Morris, G. A.; Freeman, R. *J. Magn. Reson.* **1978**, *29*, 433−462.
(17) Subramanian, S.; Bax, A. *J. Magn. Reson.* **1987**, *71*, 325−330.
(18) Sørensen, O. W.; Rance, M.; Ernst, R. R. *J. Magn. Reson.* **1984**, *56*, 527−534.
(19) Davis, D. G. *J. Magn. Reson.* **1989**, *81*, 603−607.
(20) Marion, D.; Bax, A. *J. Magn. Reson.* **1988**, *79*, 352−356.
(21) Rance, M. *J. Magn. Reson.* **1987**, *74*, 557−564.
(22) Kessler, H.; Griesinger, C.; Kerssebaum, R.; Wagner, K.; Ernst, R. R. *J. Am. Chem. Soc.* **1987**, *109*, 607−609.
(23) Dezheng, Z.; Toshimichi, F.; Nagayama, K. *J. Magn. Reson.* **1989**, *81*, 628−630.
(24) Govil, G.; Hosur, R. V. In *NMR. Basic Principles and Progress*; Diehl, P., Fluck, E., Kosfeld, R., Eds.; Springer: Berlin, 1982; Vol. 20, pp 1−216.

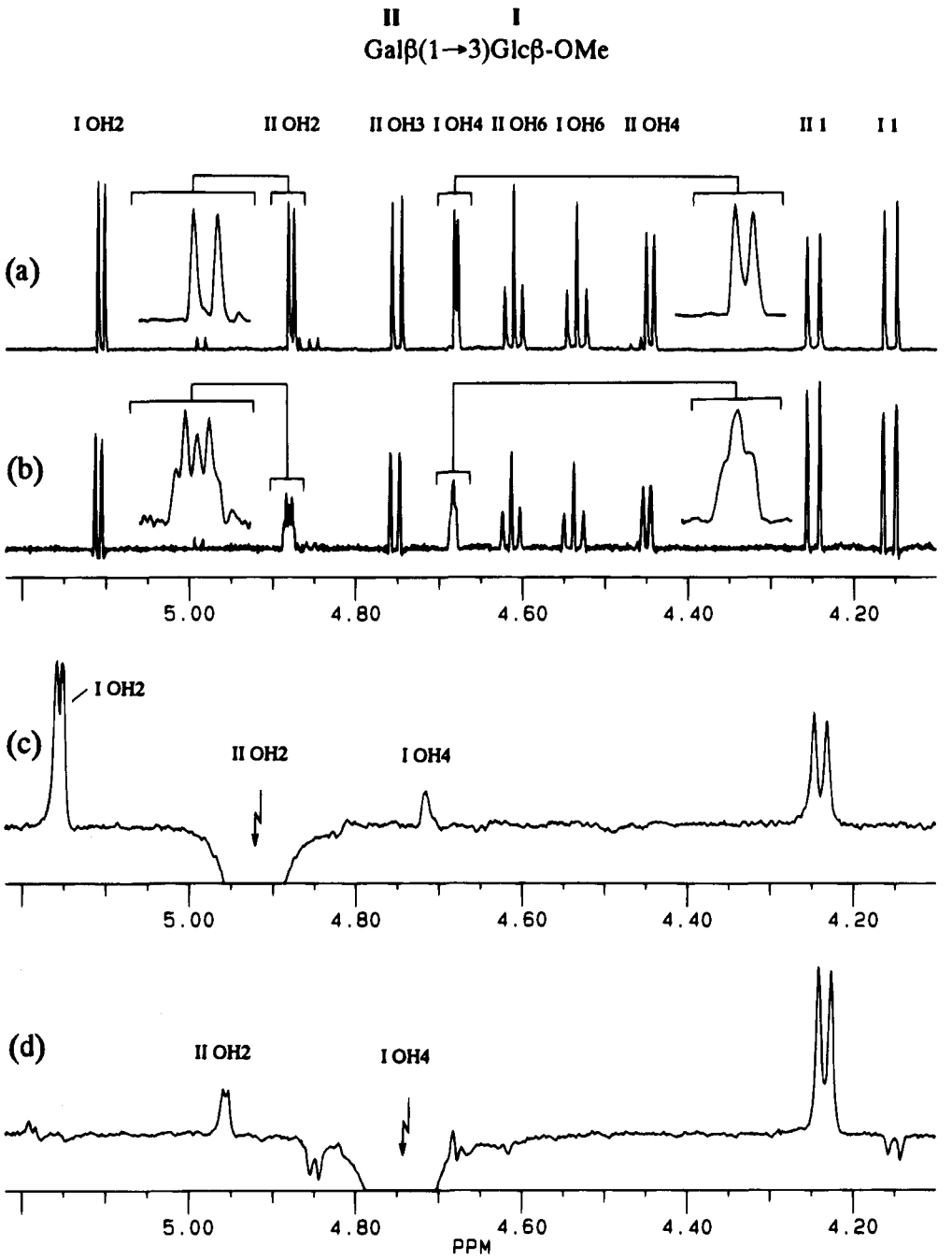

Figure 1. (a) Hydroxyl and anomeric protons region of a 500 MHz ^{1}H NMR spectrum of the title disaccharide **1** in Me_2SO-d_6 at 306 K. The insets show expansions of the Gal-II OH2 and Glc-I OH4 proton signals. (b) As in (a), with partially deuterated hydroxy groups (H:D ≈ 55:45). (c, d) ROESY difference spectra obtained with selective excitation of the II OH2 and I OH4 protons at 296 and 290 K, respectively.

basis of the $^3J_{HOCH}$ constant (Table 1) and relative NOEs to neighboring C-linked protons of the same sugar residue. The plot of a H···H distance in the Φ,Ψ coordinate system encircles an area in the conformational space where this conformation dwells. The equilibrating conformation(s) with longer distances for the same proton pair are neglected, although they may be determinable by distance constraints found for other proton pairs. Hydrogen bond constraints of 3.0 Å are plotted similarly, the lower limit being set at 2.7 Å.[11] A restricted area of overlap delimited by two or more contours is considered to define a conformer with a probability increasing with the number of contours contributing to this overlap. If *these same* contours overlap in another area, this can but does not necessarily mean that two conformations exist. In this case, energy-minimum calculations can indicate which of the three alternatives (conformation *a* and/or *b*; *a*, *b* are arbitrary labels) holds. If however, a second area of Φ,Ψ space is delimited by one or more contours referring to other constraints, clearly two conformations can be expected to exist. We call the first type of contours compatible, and the second exclusive.[13]

The interproton distances were calculated by using the expression $r_{kl} = r_{oij}(V_{oij}/V_{kl})^{1/6}$, where V_{oij} and r_{oij} are the cross-peak volume and distance for the reference interaction. Cross-peak volumes were calculated by using Bruker software integration routine and corrected for offset effects. Although the ROESY pulse sequence applied effectively reduces the Hartmann−Hahn magnetization transfer, several 1D ROE spectra were recorded with three different offset values of the spin-lock frequency each in order to ascertain that the observed ROEs are indeed not affected by such a transfer.[8a] The integral intensities of all nonoverlapped ROE signals were found constant within the limits of experimental errors.

Molecular Mechanics Calculations. The RAMM program[25] based on the MM2-87 force field[26] was used to calculate the

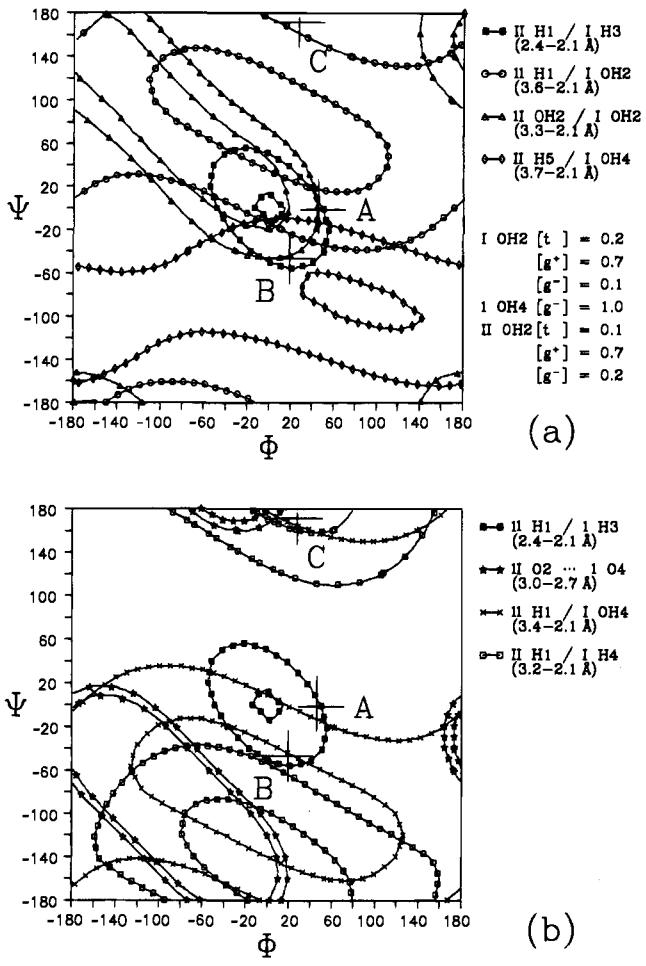

Figure 2. NOE and hydrogen bond constraints for **1** plotted in Φ,Ψ coordinates. Numbering of sugar residues (Roman numerals) and protons or oxygens in each of the residues (Arabic numerals), as in Figure 1 and Table 1. Distance limits for the pairs of contours, and the role of rotamer populations are explained in Methods. The Φ,Ψ coordinates of the lowest-energy conformations A, B, and C (*cf.* Table 2 and Figure 3) are marked with large crosses.

Table 1. Chemical Shifts, δ (ppm from Me_4Si), Coupling Constants, *J*(Hz), and Temperature Coefficients, κ(-10^3 ppm/°C) for Methyl 3-β-D-Galactosyl-β-D-glucopyranoside (**1**) in Me_2SO-d_6 at 303 K

	II Galβ1			⟶	I 3Glcβ1-OMe		
proton	δ	*J*	κ		δ	*J*	κ
H1	4.247	7.6			4.153	7.8	
H2	3.393	9.5			3.159	9.0	
H3	3.336	3.1			3.325	~8.5	
H4	3.605	~0.7			3.186	9.6	
H5	3.443	~10			3.177	~6.7	
H6	~3.50	~12[a]			3.463	11.8[a]	
H6′	~3.50	~5.8[b]			3.673	1.7[b]	
Me					3.396		
OH2	4.887	3.3	4.8		5.109	3.9	5.5
OH3	4.753	5.6	6.7				
OH4	4.451	4.6	5.6		4.681	2.0	4.2
OH6	4.616	5.3	4.8		4.534	5.9	6.0

[a] $^2J_{66'}$. [b] $^3J_{5,6'}$.

conformational energy profiles. Lone electron pairs were explicitly included for all oxygen atoms, and a value of $\epsilon = 4$ for the dielectric constant was used to calculate the electrostatic energy contribution. Grid search was performed in 20° steps. For each of the Φ_i, Ψ_i values a 1000 random configurations with different orientations of pendent groups (−OH and $-CH_2$-OH) were generated, and the configuration of lowest energy was selected for the optimization. First, all internal coordinates, except for Φ and Ψ, were optimized, and the conformational energy map thus obtained was visualized and checked for minima with the aid of the SURFER program (Golden Software, Inc., Golden, CO 80402, U.S.A.). The minima selected on the map were further optimized, the Φ,Ψ angles being also released. Several conformers, some with close Φ,Ψ values, were obtained; for their final grouping based on the *rms* values of their Cartesian coordinates, the CLUSTER analysis program (own software) was used.

Molecular Dynamics Simulations. The geometry for the lowest-energy conformer from the RAMM calculation was input to run MD simulations in the Consistent Valence Force Field (CVFF)[27] with the aid of the INSIGHT II 2.1.2 and DISCOVER 2.80 modeling software of Biosym Technologies (San Diego, CA 92121-2777, U.S.A.). Simulations were carried out at 400 K, with 1 fs integration time, 250 fs intervals for data saving, 50 ps equilibration, and 1 ns data collection times. The ANALYSIS module of INSIGHT II was applied to show the time-dependence of the molecular parameters (temperature, energy, and geometry variables) in 1 ps time steps. For the statistical analysis of the MD trajectories, the DISANA program (own software), transferred to the AIX environment of the IBM RISC 53H computer, was applied. All heavy numeric calculations were performed on this computer, and for the final figure processing an AT 486 computer was used.

Results and Discussion

The ^1H chemical shifts and coupling constants for the title disaccharide **1** are presented in Table 1, and the spectrum region displaying the anomeric and hydroxyl proton signals is shown in Figure 1a. All signals of secondary hydroxy groups are sharp doublets, and those of the two primary hydroxyls are sharp triplets. Figure 1b shows the same region recorded after the hydroxyl protons have been exchanged for deuterium in the proportion of H:D ≈ 55:45. The signals of the Glc-I OH4 and Gal-II OH2 groups are clearly split, whereas all other hydroxyl signals remained unaffected. This is a convincing demonstration of the isotope effect transmitted through a hydrogen bond between the I OH4 and II OH2 groups. The engagement of these groups in hydrogen bond formation is in accord with their $^3J_{HOCH}$ coupling constants of 2.0 and 3.3 Hz, which strongly deviate from the value of 5.5 Hz characteristic of freely rotating hydroxy groups (Table 1), and hence indicate some fixed constellation. The slightly lower temperature dependence of the I OH4 and II OH2 chemical shifts (as compared with that for other secondary OH groups; Table 1) is also in agreement with this structural feature. Furthermore, the proximity of the I OH4 and II OH2 protons was revealed independently by the 1D difference ROE spectra obtained with selective excitation of either of these protons (Figure 1c,d). Since, however, ROEs are liable to artifacts of different kinds,[8a,d] it is expedient to exclude all other possible mechanisms for the generation of this crucial ROE.

The most insidious source of possible misinterpretations is ROE relayed by HOHAHA or chemical exchange, because the false signals observed for distant protons are of the same phase as the genuine signals for proximate protons. In the present context, a ROE relayed from II OH2 to the remote I OH4 in

(25) Kožár, T.; Petrák, F.; Gálová, Z.; Tvaroška, I. *Carbohydr. Res.* **1990**, *204*, 27−36.
(26) Allinger, N. L.; Kok, R. A.; Imam, M. R. *J. Comput. Chem.* **1988**, *9*, 591−595.
(27) (a) Hagler, A. T.; Huler, E.; Lifson, S. *J. Am. Chem. Soc.* **1974**, *96*, 5319−5327. (b) Hagler, A. T.; Lifson, S.; Dauber, P. *J. Am. Chem. Soc.* **1979**, *101*, 5122−5130.

the *syn* conformation (Figure 4a) could imitate a true ROE for these protons in an nonexistent *anti* conformation (Figure 4b). The possibility of ROE-relayed ROE should also be taken into account. Following Farmer et al.,[28] we will use for brevity the shorthand notation **RH** (or **HR**), **RE** (or **ER**), and **RR** for the relayed transfer of the ROE-HOHAHA, ROE-exchange, and ROE-ROE type, respectively. In 1D ROE difference spectra, the sign of the signal of the inverted spin is (−), direct ROE is positive, the **H** and **E** steps leave the respective signs unchanged, and **RR**-type relays lead to peaks having sign $(-1)^{m+1}$, where m is the number of ROE transfers.

Considering the ROE experiment with inverted spin II OH2 (Figure 1c) it is important to notice the positive phase of the anomeric II H1 signal, which shows that the formally possible {II OH2}(−) → **H** → II H2(−) → **H** → II H1(−) transfer either does not take place, or is outweighted by the {II OH2}(−) → **R** → II H1(+) direct ROE. Furthermore, the positive I H3 signal, visible in the high-field part of the spectrum not shown in Figure 1c, demonstrates that the formally possible three-spin effect, {II OH2}(−) → **R** → II H1(+) → **R** → I H3(−), either does not occur or is overbalanced by the {II OH2}(−) → **R** → I H3(+) direct ROE. In full analogy, the positive II H1 and I H3 signals observed in the experiment with inverted I OH4 spin (Figure 1d) prove that the formally feasible {I OH4}(−) → **H** → I H4(−) → **H** → I H3(−) and {I OH4}(−) → **R** → I H3(+) → **R** → II H1(−) transfers are not operative here. The exclusion of the two **H** transfer routes just discussed renders any false **H**-mediated relayed ROE between I OH4 and II OH2 impossible. It should be added that these routes were extremely improbable for one more reason: they both include a **H** step for protons strongly differing in resonance frequencies (by 975 and 747 Hz, respectively). Such protons experience quite different spin-lock field strengths and hence do not match the condition for a HOHAHA transfer in a ROESY experiment. A **R**-mediated transfer *via* I H3 and/or II H1 is also out of question, since, with $m = 2$, it would generate a negative signal instead of the positive one observed.

A misleading {II OH2}(−) → **R** → I OH2(+) → **E** → I OH4-(+) **E**-mediated transfer can also be ruled out. Indeed, signals arising from direct exchange with the inverted II OH2 would be negative, but no negative peaks are present in this spectrum (Figure 1c); hence, there is no reason to assume that the ROE-enhanced (positive) I OH2 does exchange with I OH4. Furthermore, neither a 2D ROESY spectrum nor Figure 1d show any I OH4 → I OH2 exchange. In the experiment with inverted I OH4 (Figure 1d), the only positive OH signal is for II OH2, hence this must be a genuine ROE, because there is no source from which to generate a false one for the II OH2 proton.

Thus, a short I OH4/II OH2 distance was revealed both by the hydrogen bond-transmitted H/D isotope effect and by the NOE. Whereas any NOE-determined distance can by its nature be an averaged value, an unequivocally established hydrogen bond provides straightforward evidence for the proximity of the hydroxy groups involved and a by far more precise assessment of the distance between them. Consequently, the hydrogen bond constraint was used for distance mapping, the limits for the O···O distance being set at 2.7−3.0 Å, which is a typical length of hydrogen bonds in alcohols.[11] In Figure 2 this and six NOE constraints are divided for clarity into two groups; the familiar elliptical contour for the anomeric/aglyconic II H1/I H3 proton pair, which is characteristic of one or more *syn* conformations, is drawn in both parts a and b of Figure 2. The coordinates of three lowest-energy conformations listed in Table 2 are also marked in both parts of Figure 2.

(28) Farmer II, B. T.; Macura, S.; Brown, L. R. *J. Magn. Reson.* **1987**, *72*, 347−352.

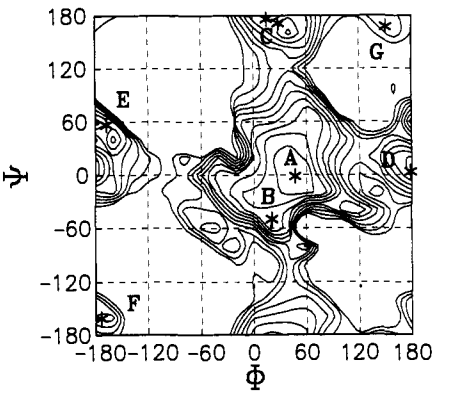

Figure 3. Relaxed conformational energy map for **1** (MM2-87 force field,[25] a RAMM calculation[24]). Energy levels are separated by 1 kcal/mol. Relaxed lowest-energy conformers are marked with asterisks and labeled according to Table 2.

In Figure 2a, the minima A and B are located within the II H1/I H3 contour and at the perimeter of the II OH2/I OH2 one. The II H1/I OH2 and II H5/I OH4 contours are in agreement with the existence of two *syn* conformations, in that they encircle the minima A and B, respectively.

The narrow II O2/I O4 hydrogen bond constraint covers an area far away from the region just discussed, hence it is obviously of the exclusive type (Figure 2b). Although it passes through a great variety of formally (geometrically) possible Φ,Ψ combinations, only those of $\Phi \approx 0°$, $\Psi \approx 180°$ or $\Phi \approx 180°$, $\Psi \approx 0°$ are located in the regions of relatively low energy (*cf.* minima C and D in Figure 3). The steep increase of the potential energy outside of these regions virtually excludes other geometries compatible with this constraint. Although the minimum C lies outside of this contour by a few degrees, this small discrepancy is of no concern, because the MM-calculated geometry is fully optimized, whereas contour plotting is performed with a disaccharide built of monosaccharides basically in their solid state geometry,[29] and with the standard value $\tau = 117°$ for the glycosidic bond angle (this might also be the reason for other discrepancies of the order of 10° in Φ and Ψ). The II H1/I OH4 constraint is compatible with both this hydrogen bond and the conformer B, hence it is inconclusive with respect to the *a* and/or *b* alternatives discussed in Methods. The last contraint is the II H1···I H4 distance of 3.2 Å. Since this distance amounts to 4.5, 3.7, and 2.1 Å in conformations A, B, and C, respectively, the average value of 3.2 Å seems to point to a considerable contribution of conformer C to the equilibrium mixture.

The conformations described by molecular dynamics (MD) simulations correspond well with the above experimental and computational results. The 1 ns simulation (Figure 5), started with the geometry of the conformer A, shows a reversible transition to conformer's C geometry and a short excursion into the region of conformer D. Most of the time the trajectories oscillate within limiting values of Φ and Ψ that embrace both conformers A and B. This run and the small energy difference between these two (Table 2) suggest oscillations between states separated by very low energy barriers within an extended energy valley (*cf.* Figure 3). The II O2···I O4 distance trajectory (Figure 5c) oscillates around the distances of ca. 5.5 (corresponding to conformations A and B), 3.5, and 2.9 Å. As the frequency distribution curve shows, the value of 2.9 Å represents a small, nevertheless appreciable population of the hydrogen-bonded conformer C. The 3.5 Å distance would then be interpretable as corresponding to a similar conformation, but

(29) (a) Cambridge Crystallographic Data Bank. (b) Lieth, C.-W. v. d.; Schmitz, M.; Poppe, L.; Hauck, M.; Dabrowski, J. In *Software-Entwicklung in der Chemie 3*; Gauglitz, G., Ed.; Springer: Berlin, 1989; pp 371−378.

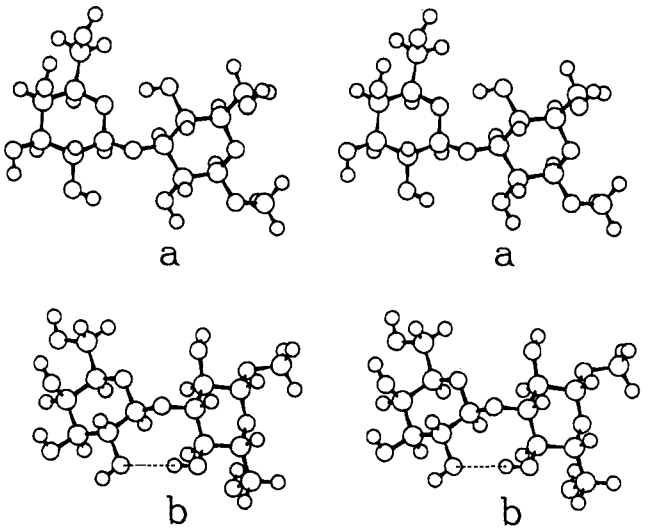

Figure 4. Stereo diagrams of (a) conformer A and (b) the lower-energy conformer C (*cf.* Figure 3 and Table 2); the I OH4••II O2 hydrogen bond is indicated by a dotted line.

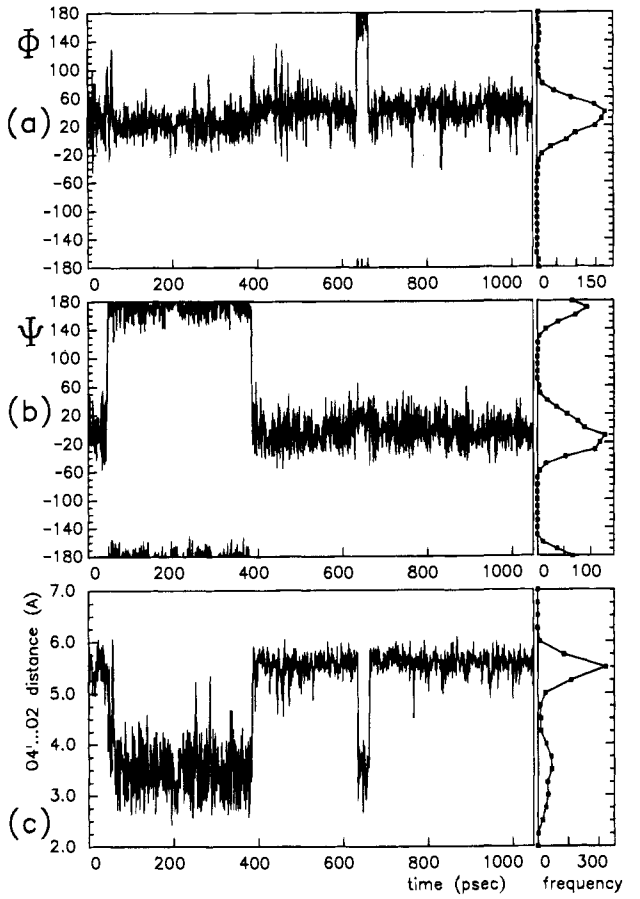

Figure 5. MD histories of the (a) Φ and (b) Ψ torsion angles and (c) the I O4••II O2 distance, simulated at 400 K with $\epsilon = 1$. The distribution curves on the right show the relative frequencies of the occurrence of the Φ,Ψ and Å values.

with the hydrogen bond disrupted. It should be emphasized that, no matter how fast the kinetics of the formation/disruption of the hydrogen bond, the deuterium isotope effect will be observable in equilibrating systems of this type unless *the H/D exchange* is fast on the NMR time scale (for a contrasting view, see ref 12c). The good agreement between the results obtained with the use of the two different methods, MM and MD, and two different force fields is illustrated in Figure 6. On the other hand, Yan and Bush[2f] performed a MD simulation for the same molecule with the use of Rasmussen's force field[7a] and observed

Table 2. Lowest-Energy Conformers of the Title Disaccharide **1**[d]

conformation	Φ^a	Ψ^a	$\tau^{a,b}$	ΔE^c
A	46.4	−1.5	115.4	0.00
B	20.7	−49.8	116.6	0.60
C(a)	28.3	171.4	117.7	2.25
C(b)	15.2	175.9	117.3	3.23
D	178.2	3.6	117.5	2.81
E	−167.5	56.3	120.2	3.25
F	−173.4	−161.3	122.2	6.70
G	150.7	167.4	121.9	8.57

[a] Angles in degrees. [b] Glycosidic bond angles. [c] Relative energies in kcal/mol. [d] MM2 − 87 Force Field, a RAMM[25] Calculation; dielectric constant $\epsilon = 4$.

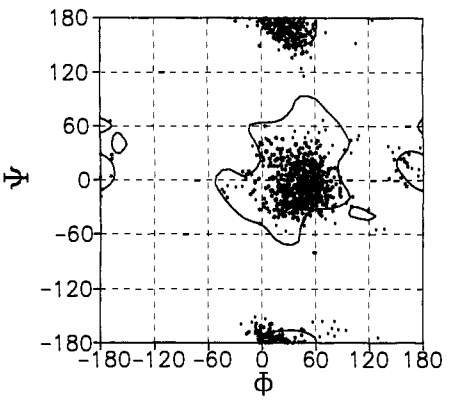

Figure 6. Distribution of the momentary conformations occurring during the MD simulation (*cf.* Figure 5a,b). The border line of 5 kcal/mol is taken from the energy map (Figure 3).

a different *anti* conformation. Although no numerical data were given, the values of $\Phi \approx 160°$ and $\Psi \approx 20°$ ($\Phi \approx 40°$ and $\Psi \approx -100°$ with the Φ,Ψ definitions used by these authors), which roughly correspond to our D conformation (Table 2), could be read from the history diagrams. Unfortunately, it seems hardly possible to discriminate between the two *anti* conformations on experimental grounds.

Conclusions

Reliably identified *anti* conformers demonstrate maximum flexibility of disaccharides and disaccharide segments of oligosaccharides. We have shown that a hydrogen bond exists in the title disaccharide between the glucose OH4 and galactose OH2 groups, this being possible only in the *anti* conformation.

Although hydrogen bonds can often be observed indirectly, e.g., by temperature dependence of hydroxyl protons' chemical shifts, the isotope effect on chemical shifts of these protons directly proves the existence of such bonds. Their length is the only nonaveraged structural constraint derived with the aid of NMR—in contrast to NOE, relaxation times, coupling constants, and chemical shifts, which describe averaged, virtual conformations.

The experimentally established coexistence of *syn* and *anti* conformations offers an opportunity to verify the ability of force fields to reproduce such situations.

Acknowledgment. T.K. acknowledges the Max Planck Society for a fellowship and the European Union for a "GO-WEST" research grant, and N.E.N. wishes to thank the International Science Foundation (Soros Foundation) for financial support.

JA942965M